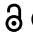



ORIGINAL RESEARCH

 OPEN ACCESS 

LCVM infection generates tumor antigen-specific immunity and inhibits growth of nonviral tumors

Camille Jacqueline^a, Matthew Dracz^a, Jia Xue^a, Robert J. Binder^a, Jonathan Minden^b, and Olivera Finn^a

^aDepartment of Immunology, University of Pittsburgh School of Medicine, Pittsburgh, PA, USA; ^bDepartment of Biological Sciences, Carnegie Mellon University, Pittsburgh, PA, USA

ABSTRACT

Antibodies and T cells specific for tumor-associated antigens (TAA) are found in individuals without cancer but with a history of infections and are associated with lowered cancer risk. We hypothesized that those immune responses were generated to transiently abnormally expressed self-antigens on infected cells (disease-associated antigens, DAA) and later on tumor cells as TAA. We tested this hypothesis in mice with a history of infection with lymphocytic choriomeningitis virus (LCMV) Armstrong strain (Arm) that causes acute infection when injected intraperitoneally or CL-13 strain that establishes chronic infection when injected intravenously. Both elicited antibodies and T cells that recognized DAA/TAA on infected cells and on mouse tumors. When challenged with those tumors, Arm-experienced mice controlled tumors better than CL-13-experienced mice or infection-naïve mice. We characterized 7 DAA/TAA that were targets of LCMV-elicited antitumor immunity. We then vaccinated mice with tumor-derived gp96, a heat shock protein that binds a variety of TAA peptides, including those expressed on virus-infected cells as DAA. Tumor-gp96 vaccine induced DAA/TAA-specific immunity. When challenged with CL-13, the mice showed lower viral copy numbers both early (day 7) and late (day 70) in infection. DAA/TAA may be immunogenic and safe candidates to develop vaccines to control both infections and cancer.

ARTICLE HISTORY

Received 11 October 2021
Revised 7 January 2022
Accepted 7 January 2022

KEYWORDS



Tumor antigens; ELISPOT; antibody responses; gp96; DIGE


Introduction

Recent successes of cancer immunotherapies designed to overcome immune tolerance to tumors and/or to produce adaptive anticancer responses leading to tumor control or elimination have not only elucidated the importance of antitumor immunity but also highlighted their limitations in advanced cancer lesions.¹ Therefore, a reasonable anticancer strategy should be developed, in addition to immunotherapy, to strengthen immunosurveillance prior to cancer occurrence, thus avoiding cancer editing and escape.² This is best accomplished with preventative cancer vaccines that have been shown to be effective for virally caused tumors.³ The choice of antigens to target with preventative cancer vaccines is critically important for their efficacy and safety. While tumors express dozens of mutated proteins that could be tumor-specific antigens (TSA), spontaneous immunity to these epitopes has not been found in cancer patients as often as it could be expected from their frequency.⁴ Instead, the majority of spontaneous antitumor immune responses are directed against nonmutated self-antigens called tumor-associated antigens (TAA). They include differentiation antigens with a tissue-specific expression such as carcinoembryonic antigen (CEA),⁵ prostate-specific antigen (PSA),⁶ or melanA/melanoma-associated antigen recognized by T cells (MART-1)⁷ and overexpressed antigens such as mucin 1

(MUC1),⁸ cyclin B1,⁹ human telomerase reverse transcriptase (hTERT),¹⁰ human epidermal growth factor receptor 2 (HER2/neu), or survivin.¹¹

Vaccines based on TAA that have been tested for years for cancer therapy have not been tested for cancer prevention or interception. This is in great part due to the long-standing assumption that TAA would not elicit strong protective immunity because they are self-antigens, or if they did, this would result in autoimmunity.¹² This assumption is beginning to change as immune responses to TAA have been found in healthy individuals who have never experienced cancer, following various immunological contexts such as allergies and infections,¹³ suggesting that they are able to safely induce immunity. For instance, immunity to the tumor-associated antigen MUC1 was found in women who experienced multiple acute infectious or inflammatory events early in life and who then had a drastically reduced risk of MUC1⁺ ovarian cancer later in life, compared to women who experienced fewer such events^{14–16} and lacked anti-MUC1 immunity. The cancer protective role of acute febrile infections is further supported by epidemiological studies that showed their association with a greatly reduced lifetime risk of cancer. Indeed, case-control studies of lymphoma, stomach, colorectal, breast, and ovarian cancer found that childhood diseases such as chicken pox and pertussis, as well as repeated cold and influenza infections throughout life, significantly decreased lifetime risk for these cancers.^{17,18}

CONTACT Olivera Finn  ojfinn@pitt.edu 

 Supplemental data for this article can be accessed on the [publisher's website](#).

© 2022 The Author(s). Published with license by Taylor & Francis Group, LLC.

This is an Open Access article distributed under the terms of the Creative Commons Attribution-NonCommercial License (<http://creativecommons.org/licenses/by-nc/4.0/>), which permits unrestricted non-commercial use, distribution, and reproduction in any medium, provided the original work is properly cited.

These findings generated a new hypothesis that the observed cancer risk reduction relies on the existence of an immune memory against disease-associated antigens (DAA), self-antigens that were transiently abnormally expressed on infected or inflamed tissues, and then later on malignantly transformed tissues as TAA.¹⁵ Our first attempt to model this in mice showed that repeated infections with the flu virus generated immunity to several DAA/TAA, which when used as preventative vaccines protected from tumor challenge.¹⁹ In the current study, we used the lymphocytic choriomeningitis virus (LCMV) to explore the difference between an acute and a chronic viral infection in their cancer protection potential and also the impact of preexisting antitumor immunity on the resolution of such viral infections. LCMV Armstrong strain (Arm) produces an acute infection that resolves in 8 days, while Clone13 strain (Cl-13) causes chronic viremia that can last up to 3 months, with the virus persisting in some tissues indefinitely.²⁰ We show that mice infected with Arm develop antibodies and T cells specific for DAA abnormally overexpressed on cells of infected organs and have improved ability to later control the growth of transplantable tumors constitutively expressing some of the same DAA as TAA. Cl-13 infection did not induce tumor protection although antibodies and T cells against the same DAA/TAA were generated. According to the DAA/TAA hypothesis, TAA-specific immunity induced by a cancer vaccine should modulate not only tumor growth but also viral infections. To begin to test this, we immunized mice with mouse tumor-derived glycoprotein (gp)96, which binds a wide array of cellular peptides, including tumor-associated antigens.²¹ Gp96-peptide complexes are taken up by antigen-presenting cells (APCs) via CD91 receptor²² for cross-presentation to CD8⁺ T cells. We demonstrated that immunization with tumor-derived gp96, and not normal liver cell-derived gp96, promotes both tumor and viral control.

Materials and methods

Mice, cell lines, and virus

Six- to eight-week-old C57Bl/6 mice were purchased from the Jackson Laboratory (Bar Harbor, ME) and maintained in the University of Pittsburgh Animal Facility. All animal protocols were in accordance with IACUC guidelines at the University of Pittsburgh. LCMV-Cl-13 (Cl-13) and LCMV-Arm (Arm) strains were obtained from Dr. Rafi Ahmed, Emory University, Atlanta, and propagated and titered as described previously.²⁰ The Lewis Lung Carcinoma cell line (LLC), derived from a murine lung epithelial tumor, was obtained from ATCC (Manassas, VA, USA) and maintained in DMEM with high glucose (ATCC, 30–2002). EL4, a lymphoid tumor derived from mouse NK-T cells lymphoma, was maintained in c-DMEM media containing 10% heat-inactivated fetal calf serum (FCS), 1% non-essential amino acid, 1% encillin/streptomycin, 1% sodium pyruvate, 1% L-glutamine, and 0.1% 2-mercaptoethanol.

LCMV infection and tumor challenge

All mice were maintained in the University of Pittsburgh Animal Facility and infected in a BSL-2 animal facility. Mice received 2×10^5 PFU (200 μ L) of LCMV-Arm intraperitoneally to initiate acute infection or 4×10^6 PFU (200 μ L) of LCMV-Cl-13 intravenously to initiate chronic infection. Mice were injected with 200 μ L of PBS either intraperitoneally or intravenously to be used as controls for Arm-infected and Cl-13-infected mice, respectively. Percent weight loss was used as a measure of successful infection, and mice were weighed every other day. On day 90 or 120 after the infection by Arm and Cl-13, respectively, mice were challenged with 1×10^5 tumor cells subcutaneously in the right hind flank. The tumor length and width were measured every 2 days using calipers. Mice were sacrificed when the tumor diameter reached 20 mm, or the tumors became severely ulcerated, or otherwise advised by the University of Pittsburgh animal facility.

Gp96 vaccination

Gp96 was purified from liver lysates of normal untreated mice or from LLC tumors, as described previously.^{23,24} The purity of extracted gp96 was confirmed by Western blot (Figure S1). Mice were immunized twice, one week apart, with 2 μ g (100 μ L) of either tumor-derived or normal liver-derived gp96 injected intradermally on the ventral side, without any adjuvant. Two weeks following the second gp96 immunization, mice were either infected with Cl-13 or challenged with LLC tumors as described above. A third immunization was administered to Cl-13-infected mice at day 45 with 2 μ g (100 μ L) of either tumor-derived or normal liver-derived gp96 injected intradermally on the ventral side, without any adjuvant.

Flow cytometry

Four days before infection, sera were collected from individual mice for evaluation of preinfection antibody repertoire. Ten days postinfection, a second blood sample provided sera for postinfection antibody assays. The same procedure was followed for control PBS-injected mice. Sera were diluted at 1:60 in PBS. 1×10^5 LLC or EL4 tumor cells were plated in a 96-well plate and stained with a viability dye (1:1000 dilution in PBS, Ghost Red 780, #13-0865, TONBO Biosciences, San Diego CA, USA). After washing, cells were stained on ice for 1 hour with 60 μ L of the diluted pre- or postinfection sera. Cells were then stained on ice for 30 minutes with FITC-conjugated goat anti-mouse IgG (1:100, Invitrogen, Carlsbad, CA, USA) as the secondary antibody. Samples were run on a Fortessa flow cytometer, and 30,000 events were recorded. Controls for nonspecific background included live/dead stained LLC and EL4 cells and secondary antibody only staining for each cell type.

Immunoprecipitation of tumor antigens by pre- and postinfection sera

LLC cells were collected by scraping in cold sucrose buffer (250 mM sucrose, 20 mM Hepes, 1 mM ethylenediaminetetraacetic acid (EDTA), pH 8.0). Total cell lysates were generated from confluent T125 flasks in 500 μ L of lysis buffer (100 mM Hepes, 500 mM NaCl, 1% octylphenoxy poly(ethyleneoxy)ethanol (IgePAL CA630), 1 mM EDTA, 1 mM phenylmethylsulfonyl fluoride (PMSF), 10 μ g/ml of Leupeptin and Pepstatin, 1% 3-[dimethylammonio]-1-propanesulfonate (CHAPS) followed by a 30-minute incubation on ice, 7 cycles of 30 seconds on/30 seconds off sonication (Bioruptor[®] Pico, Diagenode, Denville, NJ, USA), and centrifugation for 15 minutes at 14,000 rpm. Lysates were precleared with the addition of Protein G Sepharose beads (Sigma-Aldrich, Inc, St. Louis, MO) previously blocked with 0.1% BSA, and the mixture was incubated for 1 hour at 4°C on an orbital shaker. Protein G beads were removed by centrifugation at 1200 rpm prior to affinity purification. Protein G HP Spin Trap Columns and Buffer Kits (GE Healthcare UK) were used following the manufacturer's protocol with the following modifications: preinfection and postinfection sera were pooled separately from mice ($n = 6$) and each set of sera was passed over 5 protein G columns (100 μ L per column); columns were washed with the binding buffer and 50 mM dimethyl pimelimidate dihydrochloride (DMP) was added to covalently cross-link the bound antibodies from each set of sera to the protein G columns, as described in the manufacturer's protocol. This was done to ensure that only the bound protein fractions were eluted from the columns and not the antibodies; 5 mg of LLC tumor lysate was then added to both the pre- and postinfection sera columns and incubated overnight at 4°C on an orbital shaker. The following day, the columns were washed with wash buffer and the bound proteins were eluted off the columns with 0.1 M glycine, 2 M urea, pH 2.9. Pooled proteins from the preinfection and postinfection antibody columns were concentrated, and the elution buffers were changed to 2D elution buffer (7 M urea, 2 M thiourea, 4% CHAPS, 10 mM Hepes, pH 8.0) using 5000 molecular weight cutoff (MWCO) Vivaspinn columns (Sartorius Stedim Biotech, Goettingen, Germany).

2D-DIGE and Liquid Chromatography/Mass Spectrometry (LC/MS) analysis

The immunoprecipitated proteins were subjected to 2D-Difference Gel Electrophoresis (2D-DIGE) to identify proteins largely or uniquely precipitated by postinfection sera (as showed in^{19,25}). 3 μ g of protein was reduced in 10 mM Tris (2-carboxyethyl) phosphine (TCEP, Sigma) for 60 minutes in the dark at 37°C. 10 mM CyDye DIGE Fluor Cy3- or Cy5-maleimide (Cy3-mal or Cy5-mal) saturation dyes (Cytiva, Uppsala, Sweden) diluted in Dimethylformamide (DMF), which label all available TCEP-reduced cysteines, were added to each sample for 30 minutes at 37°C. Labeling was quenched with 7 M Dithiothreitol (DTT). Labeling of the two samples was also reversed (reciprocal labeling) and run concurrently on a second 2D-DIGE gel to eliminate dye-dependent differences, constituting a technical replicate. First-dimensional isoelectric

point focusing (IEF) and second-dimensional SDS-PAGE were conducted as described (36) with the following modifications. Proteins were separated in the first dimension on 18 cm pH 3–10NL IPG strips on a Protean i12 IEF cell apparatus (Bio-Rad, Hercules, CA, USA) for 32,000 volt hours. The samples were then separated on the second dimension SDS-PAGE in 12% polyacrylamide gels in Tris-glycine-SDS running buffer (12 g of Tris (Sigma-Aldrich), 57.6 g of glycine (Sigma-Aldrich), 20 mL of 20% SDS (Bio-Rad) in 4 L dH₂O). After electrophoresis, the gels were fixed in a solution of 40% methanol and 10% acetic acid. The gels were imaged on a custom-built (Minden laboratory), fluorescent gel imager that housed a robotic spot-cutting head. The resultant fluorescence images were analyzed, and selected spots were then cut from the gels and identified via Nano LC-ESI-MS/MS, as described²⁶ with no modification. After identification, the characteristics of the proteins and their sequences were obtained through the Uniprot database (<https://www.uniprot.org>). Source Extractor, a neural network-based star/galaxy classifier run by Docker, was applied to quantify the changes in 2D-DIGE gels. Once the intensity of each spot is extracted, Cy3/Cy5 ratios are created and normalized by the mean intensity of 5 guiding spots. Guiding spots were defined as spots equally expressed in both immunoprecipitation products (appearing yellow in the gel). The ratios were log transformed to help with visualization.

Western blot

Lung and spleen tissues were homogenized with a tissue homogenizer (Tissue-Tearor, Biospec), and total lysate was obtained in 1% SDS, 1% IGEPAL, 0.5% NaDeoxycholate, 100 mM Hepes pH 8.0, following boiling for 10 minutes, 5 cycles of sonication for 30 seconds ON/ 30 seconds OFF and centrifugation at 14000 rpm for 20 minutes. The same procedure was applied to generate total cell lysate from LLC and EL4 tumor cells. Prior to Western blotting, protein concentrations were determined by BCA assay. 50 μ g of proteins were separated by SDS-PAGE and transferred to PVDF membranes (#1620177, Bio-Rad). Blots were incubated for 1 hour at room temperature with anti-gelsolin, anti-STIP1, anti-GRP75, anti-HSP60, anti-PRDX6, and β -actin antibodies (See Table S1). Blots were incubated for 1 hour at room temperature with HRP-conjugated antibodies and developed with chemiluminescence reagents (SuperSignal West Pico Substrate, cat. #34580, ThermoFisher). All Western blots were scanned on FluoroChem M (ProteinSimple, San Jose, CA, USA), and band densitometry analysis was performed on all blots using Image J (NIH, Bethesda, MD). When multiple bands were detected around the expected size, they were all integrated in the calculation. All bands were normalized according to the background signals and then against β -actin. Once normalized, all experimental bands and lanes were compared with normal tissues.

ELISA

1 μ g/ml of one of the following proteins was coated on Immulon 4HBX ELISA plates (Thermo scientific) in duplicate wells: GRP75 (human), STIP1 (mouse), HSP60 (mouse),

gelsolin (human), and PRDX6 (mouse) (Abcam). Human proteins were used, being highly conserved between mouse and humans. Duplicate wells coated with 2.5% BSA served as controls for nonspecific binding. Plates were then placed overnight at 4°C. The next day, pre- and postinfection sera were diluted 1:50 in 2.5% BSA, added to ELISA plates, and kept for 1 hour at room temperature. Plates were washed and incubated with 1:1000 dilution of antimouse IgGκ binding protein-HRP (Santa Cruz, Dallas, TX, USA). Plates were washed again, and the TMB substrate (Biolegend) was added for 15 to 30 minutes, followed by 2 N sulfuric acid to stop the developing signal. ELISA plates were read at 450 nm on a SpectraMaxi3 (Molecular Devices, San Jose, CA, USA). Data were represented using the average of duplicate antigen-coated wells.

ELISPOT

Spleens were aseptically removed 10 days after infection, and single-cell suspensions were made by the passage of the tissue through the sterile meshed after red blood cells were lysed. Multiscreen IP Filter Plates (Millipore Sigma, Burlington, MA, USA) were coated with 100 μl of 2 μg/ml of IFN-γ capture antibody (BD Biosciences) and incubated overnight at 4°C. After washing, wells were blocked with complete media for 2 hours at room temperature. Serial dilutions from 500,000 to 125,000 splenocytes were used with 2.5 μg/ml of protein and placed overnight at 37°C. The following day, wells were extensively washed and incubated with 100 μl of 1.25 μg/ml of IFN-γ detection antibody (BD Biosciences) overnight at 4°C. Finally, 1 μg/ml of streptavidin solution was added to the wells after washing and incubated for 1.5 hours at room temperature. The plates were developed by the addition of 100 μl of AEC substrate (1:50, BD Biosciences) for 30 minutes in the dark. Spots numbers were measure using an AID Classic ELISPOT Reader (AID-diagnostika GmbH, Strasberg, Germany).

RNA extraction and qRT-PCR

Total RNA was isolated from 50 μl of blood or 20 million splenocytes using Trizol according to the manufacturer's instructions. Single-strand cDNA was synthesized in a volume of 20 μL containing 2 μg of total RNA, 1 μL of random hexamer, 0.5 mM dNTPs, and 200 U of SuperScript™ IV Reverse Transcriptase (SuperScript IV First-Strand Synthesis System Kit, ThermoFisher). Synthesis of cDNA was performed according to the manufacturer's protocol with an initial step at room temperature for 10 minutes, followed by 10 minutes at 50°C and 10 minutes at 80°C in a thermocycler (Mastercycler X50s, Eppendorf, Germany). Remaining RNA was removed with an incubation at 37°C for 20 minutes with 1 μL/sample of RNase H (SuperScript IV First-Strand Synthesis System Kit). PCR amplification was performed using SYBR Green Master Mix (QIAGEN), 2 μL of cDNA as a template, and 1 μL of cDNA-specific sense (5'-CATTACCTGGACTTTGTCAGACTC-3') and anti-ense primers (5'-GCAACTGCTGTG TTCCCGAAAC -3') obtained from Integrated DNA Technologies© (Coralville, IO, USA). PCR was performed for 45 cycles at 95°C for 15 seconds and annealed at 60°C for 30 seconds in the Step One Plus

(Applied Biosystems, Foster city, CA, USA). Viral copies numbers were calculated using a standard curve based on linearized plasmid 10-fold dilutions.

Statistical analysis

Significance analyses were performed by using GraphPad Prism software version 7.0 (GraphPad Inc. San Diego, CA). Results were represented as means ± standard error of the mean (SEM) or standard deviation (SD) as specified in the legend. Statistical means and significance were analyzed using the appropriated tests as specified. Significance for all experiments was defined as following: * $p < .05$, ** $p < .01$, *** $p < .001$, and **** $p < .0001$.

Results

Acute and chronic LCMV infections in mice generate antibodies against mouse tumors, but only the acute infection controls tumor growth

Mice were injected with 2×10^5 PFU of Arm in 200 μL intraperitoneally to initiate acute infection or 4×10^6 PFU in 200 μL of Cl-13 intravenously to initiate chronic infection. Control mice were injected with 200 μL of PBS either intraperitoneally as controls for Arm infection or intravenously as controls for Cl-13 infection (Figure S2). Arm-infected mice showed only a slight decrease in the body weight during the first 10 days following infection and recovered as they cleared infection. In contrast, CL-13 infected mice lost close to 20% of their starting body weight by day 10 and were unable to recover their initial weight even after a month (Figure S3), consistent with the establishment of a chronic infection, as previously reported.²⁷ 90 days later, Arm-infected mice and their PBS controls were challenged with either Lewis Lung Carcinoma cell line (LLC) of epithelial origin or a lymphoid tumor cell line EL-4 (Figure S2). We chose two different cell tumor types to explore tissue specificity of DAA/TAA expression. LLC tumors became palpable at day 9 (Figure 1a), and EL4 at day 11 (Figure 1b). By day 12, LLC tumors in the Arm-experienced mice began to diverge from the PBS (virus naïve) control group, growing slower until day 23 when all control mice had to be sacrificed due to the large size of their tumors. The average tumor size in Arm-experienced mice was 786 mm² compared to 1,452.5 mm² in the control group. EL4 tumor growth in Arm-experienced animals started to diverge at day 14, showing at the end a smaller average tumor size (409.49 mm²) compared to control mice (699.25 mm²) (see Table S2 for growth kinetics).

Cl-13-experienced animals were challenged with tumor cell lines 120 days after the initial infection. Tumors became palpable at day 9 for both cell lines (Figure 1c and d). At day 11, LLC tumor growth kinetics between the Cl-13-experienced animals and the control group began to diverge (Figure 1c), but in this case, the tumors grew faster in Cl-13-experienced mice. On day 23, the average tumor size in Cl-13-experienced mice was 663.83 mm² compared to 472.28 mm² in the control group. EL4 tumor growth kinetics and size were the same in CL-13-experienced mice as in the controls (Figure 1d, Table S2).

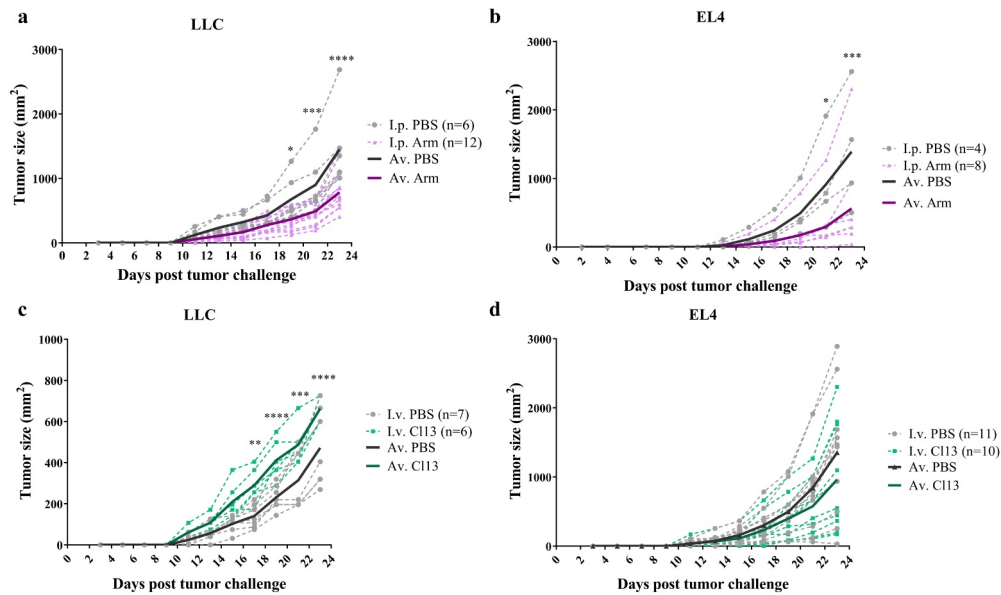


Figure 1. LCMV Arm-experienced mice control tumor growth, while LCMV CL-13-experienced mice do not. 90 days postinfection, Arm-experienced and control mice were challenged subcutaneously with 1×10^5 cells of two different tumor cell lines, LLC (a) and EL4 (b). CL-13-experienced mice were challenged 4 months postinfection subcutaneously with 1×10^5 LLC (c) or EL4 (d) tumor cells. Data are representative of two experiments per infection and per tumor type; total number of mice per group is indicated in parentheses. Sidak's test: * $p < .05$, ** $p < .01$, *** $p < .001$, **** $p < .0001$.

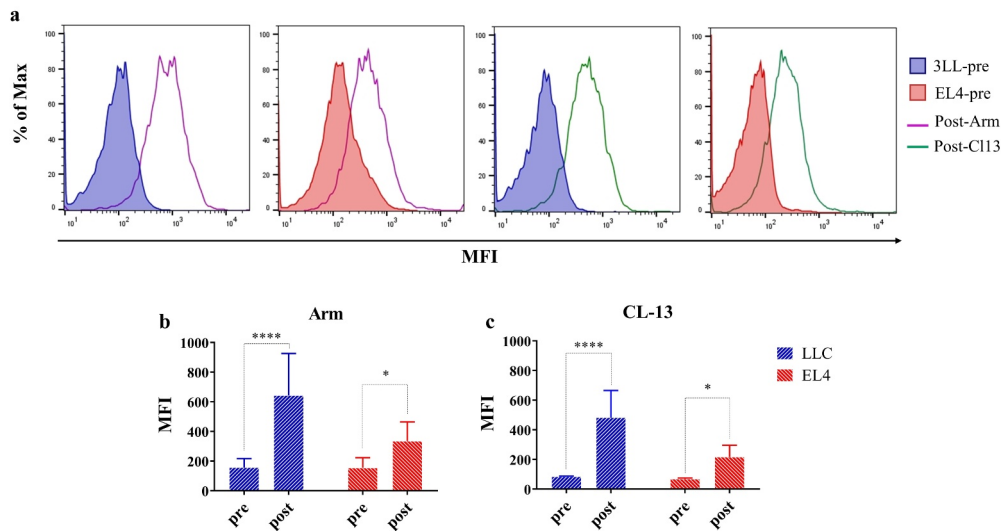


Figure 2. LCMV infection induces antibodies against molecules on the surface of cancer cells. A) Representative histograms show staining of LLC and EL4 tumor cells with sera collected four days prior to infection (pre) and 10 days after Arm and CL-13 infection (post). Results for Arm (b) and CL-13 (c)-inoculated mice are shown as an average of mean MFI ($n = 8$ for each condition) and are representative of two experiments. Error bars represent SD; Fisher LSD test: * $p < .05$, **** $p < .0001$.

Based on the hypothesis that a viral infection induces expression of DAA and subsequent immunity against these DAA expressed as TAA on tumors, we examined the pre- and postinfection sera for the ability to stain EL4 and LLC tumor cells (Figure 2a). Mean Fluorescence Intensity (MFI) measured by flow cytometry of staining of both tumor cell lines with postinfection sera was significantly higher compared to that with preinfection sera (Figure 2b and c). Such a difference was not observed in the control mice injected with PBS intraperitoneally or intravenously and from which sera were collected at the same time points as from infected mice (Figure S4).

Identification and characterization of candidate DAA/TAA

To identify molecules specifically recognized by LCMV-Arm postinfection sera, representing DAA/TAA potentially responsible for the observed antitumor immunity, LLC tumor lysate proteins were immunoprecipitated with pre- and postinfection protein-G column-purified IgG, labeled with two different Cyanine-based saturation dyes and resolved by 2D-DIGE²⁵ as described in Materials and Methods. Figure 3a shows a representative 2D gel where proteins immunoprecipitated with preinfection IgG (green) and with postinfection IgG (red) were resolved and visualized as spots. We then quantified the difference in expression by analyzing the pixel intensity of

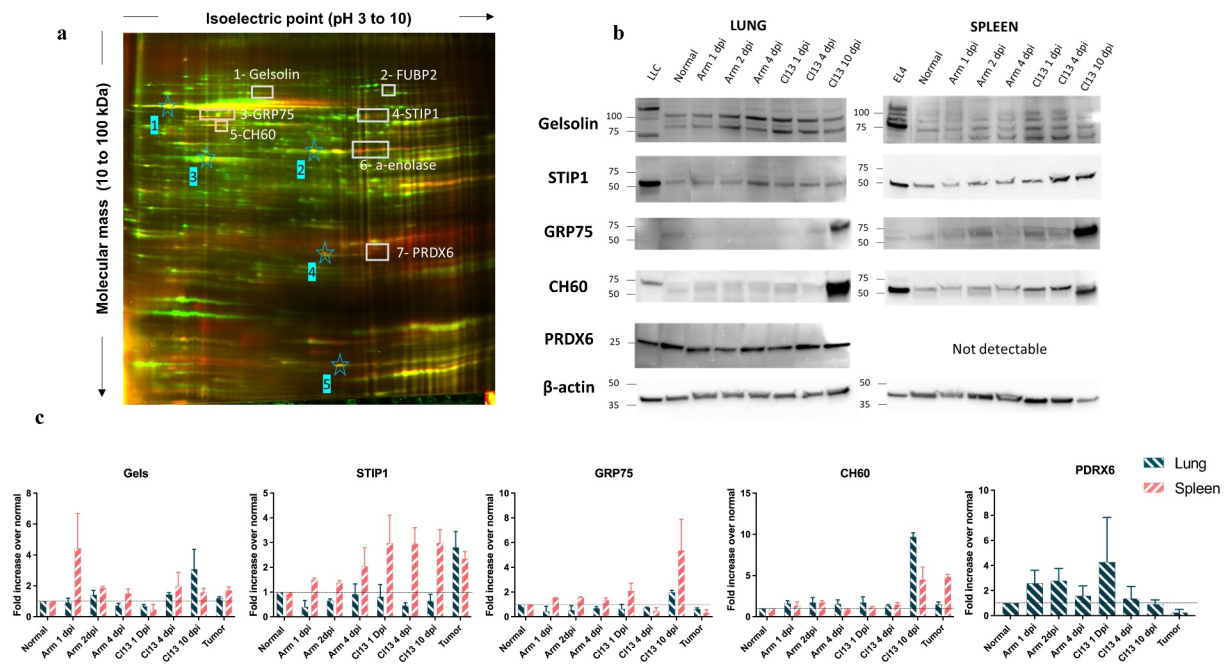


Figure 3. Postinfection sera react with specific TAA on LLC tumor that are overexpressed as DAA on infected tissues. A) Pre- and 10 days post-Arm infection sera were used to precipitate proteins from LLC tumor lysates, which were then labeled with Cy3-mal or Cy5-mal dyes and mixed and resolved on an isoelectric focusing strip with a pH gradient of 3 to 10. They were then separated according to their molecular mass. Images taken for each dye were overlaid, and differences between samples were identified. Green spots: proteins immunoprecipitated by preinfection sera; red spots: proteins immunoprecipitated by postinfection sera; yellow: proteins immunoprecipitated by both sera. White rectangles and numbers indicate 7 DAA/TAA repeatedly recognized by postinfection sera and identified by mass spectrometry. Blue stars: guiding spot for quantification. The example is representative of four technical replicates. B) Total protein lysates from lung and spleen tissues at different time points after Arm or CL-13 infection, and from tumor cells, were resolved on SDS gels and immunoblotted with antibodies against 5 of those: gelsolin, STIP1, GRP75, CH60, peroxiredoxin 6 (spots 1, 4, 3, 5, and 7 of the gel in A), and β -actin. C) Densitometry analysis performed using ImageJ. Tumor cell lines were used to approximate the expression of the DAA/TAA in spleen (EL4) and lung (LLC) tumors. Background was subtracted, and β -actin was used as a loading control to normalize each band. All lanes were compared with normal tissues. Error bars represent SEM of two independent experiments.

each spot in the images of 2D gels using a Source Extractor across 4 technical replicates (Figure S5A as an example). After normalization that accounts for differences in dye intensities, we considered that proteins were significantly differentially expressed when they had a \log_2 -fold change in spot intensity > 1 (Figure S5B). These protein spots were excised from the gel, digested into peptides with trypsin, and subjected to mass spectrometry analysis. We repeatedly found 7 proteins differentially immunoprecipitated by postinfection sera: gelsolin, FUBP2, GRP75, STIP1, CH60, peroxiredoxin 6, and α -enolase, fulfilling the criteria for DAA/TAA.

We further characterized the expression of 5 of these proteins for which antibodies were commercially available, in tumor cells and in LCMV-infected lungs and spleens by Western blot analysis. These proteins were constitutively overexpressed in both tumor cell lines, LLC and EL4, and also in lung and spleen tissues at various time points after infection with either Arm or CL-13 (Figure 3b). As previously reported,²⁸ there are multiple bands for gelsolin, the smaller molecular weight most likely to be truncated forms of the full-length molecule and the larger molecular weight form likely to be a complex with fibronectin. Postinfection sera probably reacted with different gelsolin forms in lung and spleen lysates. In Figure 3c, we show quantitative data from the Western blot. Gelsolin was overexpressed in tumor cells and in infected tissues 1 day after Arm infection and 4 to 10 days after CL-13 infection. STIP1 protein levels were elevated in tumor cells and at all time points during CL-13 infection. GRP75 was not

overexpressed in tumor cell lines, but showed high expression in the spleen at different time points after both infections. CH60 was overexpressed in EL4, in Arm-infected lungs, and in CL-13 tissues 10 days after infection. PRDX6 was only expressed in lung tissues, and protein levels were increased early after both infections.

Detection of antibodies and T cells specific for the newly identified DAA/TAA in infected animals

We used ELISA to confirm the increase of specific antibodies recognizing these individual DAA/TAA in postinfection sera compared to preinfection sera. We found that mice previously infected with either Arm or CL-13 had higher levels of anti-gelsolin and anti-CH60 IgG (Figure 4a). Anti-GRP75 and anti-PRDX6 antibodies were found at significantly higher levels in mice after Arm infection compared to preinfection levels. Anti-STIP1 antibody levels were not affected by the infections. We also tested sera post-tumor challenge to determine if tumor growth could serve as a booster of DAA/TAA-specific immunity and immune memory previously induced by the infection. Antibody titers against all DAA/TAA slightly increased after tumor challenge except for STIP1. Only two CL-13-infected mice showed a significant increase in anti-STIP1 antibody response after tumor challenge.

Interferon gamma (IFN- γ) ELISPOT assays were carried out to assess generation of T cell responses specific for DAA/TAA. In this assay, the number of spots represents the number

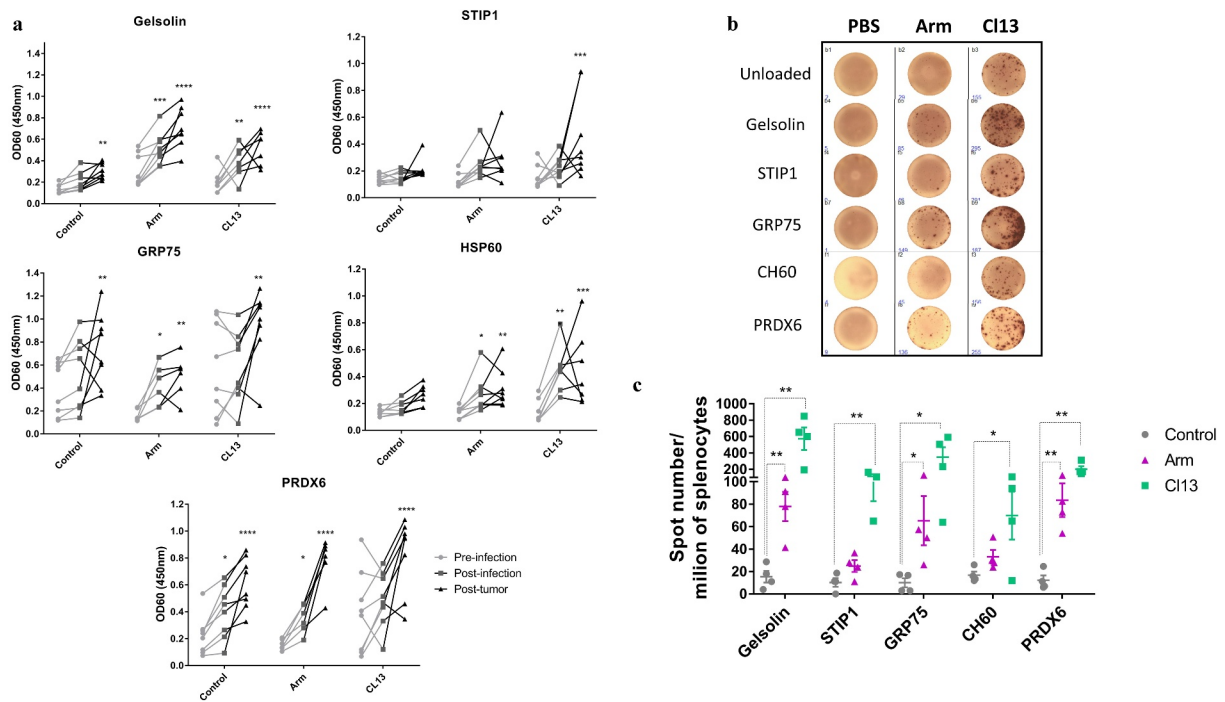


Figure 4. Both acute and chronic LCMV infections induce DAA/TAA-specific antibodies and T cells. A) Sera were collected four days prior to infection (pre), ten days after infection (post), and 23 days after tumor challenge (post-LLC), from 8 mice per group and assayed on ELISA plates on duplicate wells coated with individual proteins. Tumor cells were injected 3 months postinfection. Control mice were injected with PBS. Serum was collected at the same time points in all groups (described in Figure S2). Wells coated with 2.5% BSA served as nonspecific binding controls. Results are represented as mean optical density (OD60) and representative of two independent experiments. T-tests: * $p < .05$, ** $p < .01$, *** $p < .001$, and **** $p < .0001$. B) Ten days after infection, spleens were harvested and subjected to a 24 h IFN- γ release ELISPOT assay to determine DAA/TAA-specific T cell responses. Images are shown of wells in each group with or without stimulation. C) Quantitation of numbers of spots in each group (the same groups as in a); 4 mice per group) after the number of spots in unloaded controls was subtracted. Error bars represent SEM, T-tests: * $p < .05$ and ** $p < .01$.

of IFN- γ -producing T cells reactive to individual proteins, whereas the size of the spots represents the quantity of IFN- γ produced by a given cell (Figure 4b). Ten days after infection, Arm-experienced mice showed strong responses to gelsolin, GRP75, and PRDX6. Even stronger responses were observed in CL-13-infected mice than the same proteins and in addition to STIP1 and CH60. The responses were significantly higher than those observed with splenocytes from control mice (Figure 4c). The higher number of responding T cells in spleens of CL-13-infected mice compared to Arm-infected mice most likely is due to the Arm infection being already cleared and many DAA-specific T cells having already left the spleen and entered circulation, while CL-13 infection was still ongoing, keeping DAA-specific T cells in the spleen. We also tested the presence of DAA/TAA-specific T cells in infection-naïve mice that were challenged with LLC tumors and found an increase in IFN- γ -producing T cells specific for STIP1 and GRP75 (Figure S6).

Tumor-derived gp96 vaccine provides partial protection from tumor challenge and modulates infection with CL-13

Having shown that tumor growth can be modulated by a history of viral infections, we wanted to test if the inverse would be true and that immunity induced by tumors could modulate subsequent viral infections. We vaccinated mice with the heat shock protein, glycoprotein 96 (gp96) purified from LLC tumor cells (gp96-LLC), or control gp96 purified from normal liver cells (gp96). Gp96 binds intracellular tumor

peptides, some of which we expected to be not only from the DAA/TAA that we identified but also from other unknown antigens that might be shared between infected and malignant cells. After two injections two weeks apart, vaccine-elicited immunity was assayed, and mice were either challenged with LLC tumor or infected with CL-13 (Figure S7).

We first confirmed that the vaccine elicited responses to antigens on tumor cells by staining EL4 and LLC tumor cells with pre- and postvaccination sera and analyzing the stained cells on the Fluorescence-Activated Cell Sorter (FACS). We found that the Mean Fluorescence Intensity (MFI) of staining with postvaccination sera from gp96-LLC-vaccinated mice was significantly higher compared to prevaccination sera and sera from the gp96 control-vaccinated mice (Figure S8). We then looked for gp96-LLC vaccine-induced DAA/TAA-specific T cells in splenocytes one week after the second boost. We found increased numbers of IFN- γ -producing T cells compared to controls, primarily for gelsolin and GRP75 (Figure 5a), suggesting that peptides derived from these DAA/TAA were carried by gp96 extracted from tumor cells and cross-presented to T cells.

We then measured the protective potential of the gp96-LLC vaccine against tumor challenge. The two growth curves began to separate by day 16, and Gp96-LLC-vaccinated mice had significantly smaller LLC tumors by day 24 and until the end of the experiment, compared to normal control gp96-vaccinated mice (Figure 5b, Table S3). The same delay in tumor progression was observed in vaccinated mice challenged

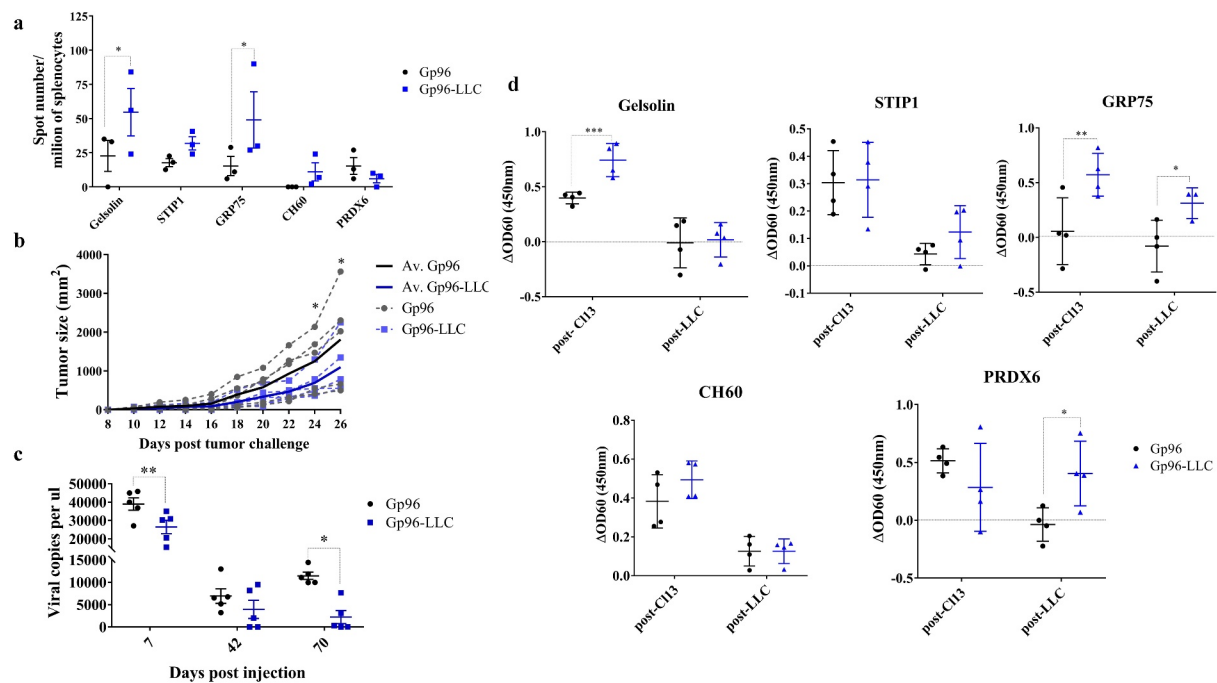


Figure 5. LLC-derived gp96 vaccine promotes tumor and virus control. A) Ten days after vaccination, spleens were harvested and subjected to a 24 h IFN- γ release ELISPOT assay to determine DAA/TAA-specific T cell responses. Numbers of spots in each group (3 mice per group) were quantified, and the number of spots in unloaded controls was subtracted. Error bars represent SEM, T-tests: * $p < .05$. B) Vaccinated animals were challenged subcutaneously with 1×10^5 of LLC tumor cells and tumor size measured every other day. Sidak's test: * $p < .05$. C) Viral copies in the blood or in the spleen (70 days after CL-13 infection) were assessed by qRT-PCR using specific primer for the GP viral protein at different time points after CL-13 infection. Each sample was run in duplicates. Error bars represent SEM, Fisher LSD test: * $p < .05$ and ** $p < .01$. D) Sera were collected four days prior to infection, 23 days after infection (post), and 23 days after tumor challenge (post-LLC) from 4 mice per group and assayed on ELISA plates on duplicate wells coated with individual DAA/TAA. Wells coated with 2.5% BSA served as nonspecific binding controls. Results are represented as mean optical density (OD) after OD from preinfection sera (dashed line) was subtracted and are representative of two independent experiments. Error bars represent SEM, T-tests: * $p < .05$, ** $p < .01$, and *** $p < .001$.

with EL4 (Figure S9). We also evaluated the vaccine's potential to control CL-13 infection by measuring the number of viral copies in the blood or in the spleen at different days after infection. There was a significantly lower number of viral copies in the blood at day 7 and in the spleen at day 70 (after the third immunization) in the group previously vaccinated with gp96-LLC (Figure 5c).

Finally, we tested if in gp96-vaccinated mice, antibody responses against our specific DAA/TAA were further boosted after being challenged with either CL-13 infection or LLC tumor. Levels of anti-gelsolin and anti-GRP75 antibodies were indeed higher in vaccinated mice following CL-13 infection, while the tumor challenge boosted anti-GRP75 and anti-PRDX6 antibody titers (Figure 5d).

Discussion

The data presented here add an immune mechanism to other postulated mechanisms of natural protection against cancer and the positive role of history of acute infections in reducing lifetime cancer risk.^{13,19,29–32} We show that this protective effect is likely mediated through the generation of immune responses and memory to transiently aberrantly expressed self-molecules that are shared by infected cells and cancer cells. We used here a model infection of mice with two strains of the same virus, LCMV-Arm that causes acute infections and LCMV-CL-13 that establishes a chronic

infection. Both acute and chronic LCMV infections induced antibodies and T cells against self-molecules abnormally expressed in infected cells as DAA and in tumor cells as TAA, but only the acute infection generated tumor-protective immunity. This result was somewhat expected. DAA/TAA-specific T cells generated at the beginning of the infection would have had a chance to mature into memory cells in the acute infection setting where the virus is cleared in as few as 8 days. Re-expression of these antigens on the tumor would have triggered that memory response and engaged the T and B cells in tumor control. In a chronic infection, antigen-specific T and B cells generated at the start of the infection would have continued to be chronically stimulated by the antigens continuously present on infected cells, which would have created exhausted T cells by the time of the tumor challenge. We did observe a higher number of CD8⁺ T cells that were also positive for exhaustion markers Tim3 and PD-1^{33,34} in the CL-13 group splenocytes post-tumor challenge (Figure S10).

We previously showed a cancer protective role of flu infections in mice;¹⁹ however, LCMV infections may be particularly relevant for supporting our hypothesis on cross-protection between viral infections and cancer. It was previously reported that LCMV infection was able to protect against other viruses such as the poliovirus, the vaccinia virus, and the murine cytomegalovirus (MCMV),³⁵ with one possible mechanism being immune memory for shared DAA. In addition, using

a SEREX method, it was shown that 79% of new antibodies produced by LCMV infection in mice recognized antigens previously reported as human or mouse TAA.³⁶ We have now directly tested the role of LCMV-elicited immune memory in controlling tumor growth and confirmed that LCMV infection induces the production of antibodies against multiple antigens shared between infected cells and tumors. Focusing on five of these antigens, gelsolin, STIP1, GRP75, CH60, and peroxiredoxin 6, we showed that they were abnormally expressed in infected lungs, spleens, and mouse tumor cell lines and that in addition to IgG, LCMV infection induced antigen-specific T cells against these molecules. Previous reports have implicated the same molecules in various aspects of infection and/or cancer development. For example, gelsolin was shown to improve lung host defense against pneumonia by enhancing macrophage function.³⁷ On the cancer side, it was found that low levels of gelsolin promoted colon cancer progression and could be used as a prognostic marker.³⁸ Heat shock proteins (HSPs) such as GRP75 and CH60 are involved in many cellular processes ranging from viral infection to cancer.³⁹ Serum autoantibodies against STIP1 were studied as potential biomarkers in the diagnosis of esophageal cancer,⁴⁰ and peroxiredoxin 6 is overexpressed in multiple cancers and is considered to be a tumor promoter.⁴¹

The prediction we made based on infections eliciting safe antitumor immunity was that specific DAA/TAA vaccine-elicited immunity should also be safe and protective against tumors. We used the ultimate DAA/TAA vaccine, the peptide-binding chaperon gp96 purified from LLC tumor cells (gp96-LLC) and carrying a large load of peptides derived from tumor proteins, many of which we expected to be DAA/TAA, and found that the vaccine elicited antitumor immunity as well as specific immune responses to some of the identified DAA/TAA. The second prediction was that gp96-LLC-vaccinated mice would control viral infections better as well, due to DAA/TAA-specific immunity targeting the DAA on virus-infected cells. Because the acute Arm strain is very quickly cleared, we tested this prediction in the chronic CL-13 infection. We showed lower virus titers in gp96-LLC-vaccinated mice compared to the control gp96 group, with some mice completely clearing the virus after the third boost. Lack of autoimmune side effects in the presence of effective DAA/TAA immunity likely reflects significantly lower levels of DAA/TAA expression in normal cells, under the threshold of detection and destruction by specific immune effectors.⁴² We are currently working on the third prediction of our hypothesis, which is that anti-DAA memory elicited by an infection with one virus will protect from future viruses, already known or newly emerging.

Our findings foreshadow a different approach to vaccination, a “universal” vaccine based on a collection of DAA/TAA that can simultaneously protect against pathogens and cancer.⁴³ All vaccines are currently based on molecules made by pathogens that are unique to each pathogen, rather than on molecules shared by pathogen-infected cells. Similarly, in the cancer vaccines field, there is a strong emphasis on using mutated tumor antigens that are unique to each tumor. A vaccine for every pathogen requires time to create and to test. The SARS-2 pandemic has shown that

waiting for specific vaccines to be developed, even in record time, carries a large human and economic toll. Moreover, quickly mutating pathogens can avoid a specific vaccine-induced immunity. In the cancer vaccines field, current emphasis is on mutated antigens, which must await a cancer diagnosis (with a few exceptions when certain mutations can be predicted, such as in the Kras oncogene). In addition to the problem of having to make them for each tumor and often each patient, their therapeutic efficacy is greatly diminished due to the suppressive tumor microenvironment. Universal preventative vaccines that are not based on the immune response having to learn to recognize a new virus or a new mutation, but on predicted changes in infected cells and transformed cells, could prepare the immune system to recognize those changes, thus controlling known and emerging pathogens and impacting the long-standing cancer pandemic.

Acknowledgments

We are highly appreciative of the help and advice from Priyanka Manandhar in using LCMV viruses and from the Flow Core. This project used the Hillman Center for Biologic Imaging and Genomics Research Core that is supported in part by award P30CA047904.

Disclosure statement

O.J.F. is on External Advisory Boards of GeoVax, Biovelocita, Immodulon, IASO, and PDS Biotech.

Funding

This work was supported by the U.S. National Institutes of Health grants R35 CA210039 to O.J.F. and CA233803 to R.J.B., and the grant from the Forbeck Foundation to C.M.J.

References

- Sharma P, Allison JP. Immune checkpoint targeting in cancer therapy: toward combination strategies with curative potential. *Cell*. 2015;161(2):205–214. doi:10.1016/j.cell.2015.03.030.
- Finn OJ, Beatty PL. Cancer immunoprevention. *Curr Opin Immunol*. 2016;39:52–58. doi:10.1016/j.coi.2016.01.002.
- Paavonen J, Naud P, Salmerón J, Wheeler CM, Chow SN, Apter D, Kitchener H, Castellsague X, Teixeira JC, Skinner SR, et al. Efficacy of human papillomavirus (HPV)-16/18 AS04-adjuvanted vaccine against cervical infection and precancer caused by oncogenic HPV types (PATRICIA): final analysis of a double-blind, randomised study in young women. *Lancet*. 2009;374(9686):301–314. doi:10.1016/S0140-6736(09)61248-4.
- Robbins PF, Lu Y-C, El-Gamil M, Li YF, Gross C, Gartner J, Lin JC, Teer JK, Cliften P, Tycksen E, et al. Mining exomic sequencing data to identify mutated antigens recognized by adoptively transferred tumor-reactive T cells. *Nat Med*. 2013;19(6):747–752. doi:10.1038/nm.3161.
- Nollau P, Scheller H, Kona-Horstmann M, Rohde S, Hagenmüller F, Wagener C, Neumaier M. Expression of CD66a (human C-CAM) and other members of the carcinoembryonic antigen gene family of adhesion molecules in human colorectal adenomas. *Cancer Res*. 1997;57:2354–2357.
- Salman JW, Schoots IG, Carlsson SV, Jenster G, Roobol MJ. Prostate specific antigen as a tumor marker in prostate cancer: biochemical and clinical aspects. *Adv Exp Med Biol*. 2015;867:93–114. Springer New York LLC.

7. Seiter S, Monsurro V, Nielsen M-B, Wang E, Provenzano M, Wunderlich JR, Rosenberg SA, Marincola FM. Frequency of MART-1/MelanA and gp100/PMel17-specific T cells in tumor metastases and cultured tumor-infiltrating lymphocytes. *J Immunother* (1991). **1997**;25:252–263.
8. Vlad AM, Kettel JC, Alajez NM, Carlos CA, Finn OJ. MUC1 immunobiology: from discovery to clinical applications. *Adv Immunol*. **2004**;82:249–293.
9. Kao H, Marto JA, Hoffmann TK, Shabanowitz J, Finkelstein SD, Whiteside TL, Hunt DF, Finn OJ. Identification of cyclin B1 as a shared human epithelial tumor-associated antigen recognized by T cells. *J Exp Med*. **2001**;194(9):1313. doi:10.1084/jem.194.9.1313.
10. Hiyama E, Hiyama K. Telomerase as tumor marker. *Cancer Lett*. **2003**;194(2):221–233. doi:10.1016/s0304-3835(02)00709-7.
11. Schmidt SM, Schag K, Müller MR, Weck MM, Appel S, Kanz L, Grünebach F, Brossart P. Survivin is a shared tumor-associated antigen expressed in a broad variety of malignancies and recognized by specific cytotoxic T cells. *Blood*. **2003**;102(2):571–576. doi:10.1182/blood-2002-08-2554.
12. Finn OJ. Human tumor antigens yesterday, today, and tomorrow. *Cancer Immunol Res*. **2017**;5(5):347LP–354. doi:10.1158/2326-6066.CIR-17-0112.
13. Jacqueline C, Finn OJ. Antibodies specific for disease-associated antigens (DAA) expressed in non-malignant diseases reveal potential new tumor-associated antigens (TAA) for immunotherapy or immunoprevention. *Semin Immunol*. **2020** Apr;6:101394. doi:10.1016/j.smim.2020.101394.
14. Cramer DW, Titus-Ernstoff L, McKolanis JR, Welch WR, Vitonis AF, Berkowitz RS, Finn OJ. Conditions associated with antibodies against the tumor-associated antigen MUC1 and their relationship to risk for ovarian cancer. *Cancer Epidemiol Biomarkers Prev*. **2005**;14(5):1125–1131. doi:10.1158/1055-9965.EPI-05-0035.
15. Cramer DW, Vitonis AF, Pinheiro SP, McKolanis JR, Fichorova RN, Brown KE, Hatchette TF, Finn OJ. Mumps and ovarian cancer: moder interpretation of an historic association. *Cancer Causes Control*. **2011**;21(8):1193–1201. doi:10.1007/s10552-010-9546-1.Mumps.
16. Terry KL, Titus-Ernstoff L, McKolanis JR, Welch WR, Finn OJ, Cramer DW. Incessant ovulation, mucin 1 immunity, and risk for ovarian cancer. *Cancer Epidemiol Biomarkers Prev*. **2007**;16(1):30–35. doi:10.1158/1055-9965.EPI-06-0688.
17. Abel U, Becker N, Angerer R, Frenzel-beyne R, Kaufmann M, Wysoeki S, Schulz G. Common infections in the history of cancer patients and controls. *J Cancer Res Clin Oncol*. **1991**;117(October1987):339–344. doi:10.1007/BF01630717.
18. Parodi S, Crosignani P, Miligi L, Nanni O, Ramazzotti V, Rodella S, Costantini AS, Tumino R, Vindigni C, Vineis P, et al. Childhood infectious diseases and risk of leukaemia in an adult population. *Int J Cancer*. **2013**;133(8):1892–1899. doi:10.1002/ijc.28205.
19. Iheagwara UK, Beatty PL, Van PT, Ross TM, Minden JS, Finn OJ. Influenza virus infection elicits protective antibodies and T cells specific for host cell antigens also expressed as tumor associated antigens: a new view of cancer immunosurveillance. *Cancer Immunol Res*. **2015**;2(3):263–273. doi:10.1158/2326-6066.CIR-13-0125.Influenza.
20. Ahmed R, Salmi A, Butler LD, Chiller JM, Oldstone MB. Selection of genetic variants of lymphocytic choriomeningitis virus in spleens of persistently infected mice. Role in suppression of cytotoxic T lymphocyte response and viral persistence. *J Exp Med*. **1984**;160(2):521–540. doi:10.1084/jem.160.2.521.
21. Binder RJ, Srivastava PK. Peptides chaperoned by heat-shock proteins are a necessary and sufficient source of antigen in the cross-priming of CD8+ T cells. *Nat Immunol*. **2005**;6(6):593–599. doi:10.1038/NI1201.
22. Sedlacek AL, Younker TP, Zhou YJ, Borghesi L, Shcheglova T, Mandoiu II, Binder RJ. CD91 on dendritic cells governs immunosurveillance of nascent, emerging tumors. *JCI Insight*. **2019**;4:7. doi:10.1172/jci.insight.127239.
23. Basu S, Srivastava PK. Calreticulin, a peptide-binding chaperone of the endoplasmic reticulum, elicits tumor- and peptide-specific immunity. *J Exp Med*. **1999**;189(5):797–802. doi:10.1084/jem.189.5.797.
24. Srivastava PK. Purification of heat shock protein-peptide complexes for use in vaccination against cancers and intracellular pathogens. *Methods A Companion Methods Enzymol*. **1997**;12(2):165–171. doi:10.1006/meth.1997.0464.
25. Minden JS. Two-dimensional difference gel electrophoresis. *Methods in Molecular Biology (Clifton, N J)*. **2012**;869:287–304.
26. Balasubramani M, Nakao C, Uechi GT, Cardamone J, Kamath K, Leslie KL, Balachandran R, Wilson L, Day BW, Jordan MA. Characterization and detection of cellular and proteomic alterations in stable stathmin-overexpressing, taxol-resistant BT549 breast cancer cells using offgel IEF/PAGE difference gel electrophoresis. *Mutat Res*. **2011**;722(2):154–164. doi:10.1016/j.mrgtox.2010.08.019.
27. Stamm A, Valentine L, Potts R, Premenko-Lanier M. An intermediate dose of LCMV clone 13 causes prolonged morbidity that is maintained by CD4+ T cells. *Virology*. **2012**;425(2):122–132. doi:10.1016/j.virol.2012.01.005.
28. Haverland N, Pottiez G, Wiederin J, Ciborowski P. Immunoreactivity of anti-gelsolin antibodies: implications for biomarker validation. *J Transl Med*. **2010**;8. doi:10.1186/1479-5876-8-137.
29. Jacqueline C, Lee A, Frey N, Minden JS, Finn OJ. Inflammation-induced abnormal expression of self-molecules on epithelial cells: targets for tumor immunoprevention. *Cancer Immunology Research*. **2020**;8(8):1027–1038. doi:10.1158/2326-6066.CIR-19-0870.
30. Jacqueline C, Parvy J-P, Faugere D, Renaud F, Misse D, Thomas F, Roche B. Infection triggers tumor regression through activation of innate immunity in *Drosophila*. *bioRxiv*. **2019** Feb;17:552869. doi:10.1101/552869.
31. Vella LA, Yu M, Fuhrmann SR, El-Amine M, Epperson DE, Finn OJ. Healthy individuals have T-cell and antibody responses to the tumor antigen cyclin B1 that when elicited in mice protect from cancer. *Proc Natl Acad Sci U S A*. **2009**;106(33):14010–14015. doi:10.1073/pnas.0903225106.
32. Zitvogel L, Perreault C, Finn OJ, Kroemer G. Beneficial autoimmunity improves cancer prognosis. *Nat Rev Clin Oncol*. **2021**;18(9):591–602. doi:10.1038/s41571-021-00508-x.
33. Sakuishi K, Apetoh L, Sullivan JM, Blazar BR, Kuchroo VK, Anderson AC. Targeting Tim-3 and PD-1 pathways to reverse T cell exhaustion and restore anti-tumor immunity. *J Exp Med*. **2010**;207(10):2187–2194. doi:10.1084/JEM.20100643.
34. Das M, Zhu C, Kuchroo VK. Tim-3 and its role in regulating anti-tumor immunity. *Immunol Rev*. **2017**;276(1):97. doi:10.1111/IMR.12520.
35. Zhou X, Ramachandran S, Mann M, Popkin DL. Role of lymphocytic choriomeningitis virus (LCMV) in understanding viral immunology: past, present and future. *Viruses*. **2012**;4(11):2650–2669. doi:10.3390/v4112650.
36. Ludewig B, Krebs P, Metters H, Tatzel J, Türeci O, Sahin U. Molecular characterization of virus-induced autoantibody responses. *J Exp Med*. **2004**;200(5):637–646. doi:10.1084/jem.20040358.
37. Yang Z, Chiou TTY, Stossel TP, Kobzik L. Plasma gelsolin improves lung host defense against pneumonia by enhancing macrophage NOS3 function. *Am J Physiol - Lung Cell Mol Physiol*. **2015**;309(1):L11–L16. doi:10.1152/ajplung.00094.2015.
38. Chen Z, Li K, Yin X, Li H, Li Y, Zhang Q, Wang H, Qiu Y. Lower expression of gelsolin in colon cancer and its diagnostic value in colon cancer patients. *J Cancer*. **2019**;10(5):1288–1296. doi:10.7150/jca.28529.
39. Flachbartová Z, Kovacech B. Mortalin - a multipotent chaperone regulating cellular processes ranging from viral infection to neurodegeneration. *Acta Virol*. **2013**;57(1):3–15. doi:10.4149/av_2013_01_3.

40. Xu YW, Liu CT, Huang XY, Huang LS, Luo YH, Hong CQ, Guo HP, Xu LY, Peng YH, Li EM. Serum autoantibodies against STIP1 as a potential biomarker in the diagnosis of esophageal squamous cell carcinoma. *Dis Markers*. 2017:2017. doi:10.1155/2017/5384091.
41. Hu X, Lu E, Pan C, Xu Y, Zhu X. Overexpression and biological function of PRDX6 in human cervical cancer. *J Cancer*. 2020;11(9):2390–2400. doi:10.7150/jca.39892.
42. Jacqueline C, Dracz M, Boothman S, Minden JS, Gottschalk RA, Finn OJ. Identification of cell surface molecules that determine the macrophage activation threshold associated with an early stage of malignant transformation. *Front Immunol*. 2021;12(October): 1–13. doi:10.3389/fimmu.2021.749597.
43. Finn OJ. The dawn of vaccines for cancer prevention. *Nat Rev Immunol*. 2018;18(3):183–194. doi:10.1038/nri.2017.140.